

# Journal of Astronomical Telescopes, Instruments, and Systems

AstronomicalTelescopes.SPIEDigitalLibrary.org

## Cryogen-free operation of the Soft X-ray Spectrometer instrument

Gary A. Sneiderman  
Peter J. Shirron  
Ryuichi Fujimoto  
Thomas G. Bialas  
Kevin R. Boyce  
Meng P. Chiao  
Michael J. DiPirro  
Megan E. Eckart  
Leslie Hartz  
Yoshitaka Ishisaki  
Caroline A. Kilbourne  
Candace Masters  
Dan McCammon  
Kazuhisa Mitsuda  
Hirofumi Noda  
Frederick S. Porter  
Andrew E. Szymkowiak  
Yoh Takei  
Mashiro Tsujimoto  
Seiji Yoshida

Gary A. Sneiderman, Peter J. Shirron, Ryuichi Fujimoto, Thomas G. Bialas, Kevin R. Boyce, Meng P. Chiao, Michael J. DiPirro, Megan E. Eckart, Leslie Hartz, Yoshitaka Ishisaki, Caroline A. Kilbourne, Candace Masters, Dan McCammon, Kazuhisa Mitsuda, Hirofumi Noda, Frederick S. Porter, Andrew E. Szymkowiak, Yoh Takei, Mashiro Tsujimoto, Seiji Yoshida, "Cryogen-free operation of the Soft X-ray Spectrometer instrument," *J. Astron. Telesc. Instrum. Syst.* 4(2), 021408 (2018), doi: 10.1117/1.JATIS.4.2.021408.

# Cryogen-free operation of the Soft X-ray Spectrometer instrument

Gary A. Sneiderman,<sup>a,\*</sup> Peter J. Shirron,<sup>a</sup> Ryuichi Fujimoto,<sup>b</sup> Thomas G. Bialas,<sup>a</sup> Kevin R. Boyce,<sup>a</sup> Meng P. Chiao,<sup>a</sup> Michael J. DiPirro,<sup>a</sup> Megan E. Eckart,<sup>a</sup> Leslie Hartz,<sup>a</sup> Yoshitaka Ishisaki,<sup>c</sup> Caroline A. Kilbourne,<sup>a</sup> Candace Masters,<sup>a</sup> Dan McCammon,<sup>d</sup> Kazuhisa Mitsuda,<sup>e</sup> Hirofumi Noda,<sup>f</sup> Frederick S. Porter,<sup>a</sup> Andrew E. Szymkowiak,<sup>g</sup> Yoh Takei,<sup>e</sup> Mashiro Tsujimoto,<sup>e</sup> and Seiji Yoshida<sup>h</sup>

<sup>a</sup>NASA, Goddard Space Flight Center, Greenbelt, Maryland, United States

<sup>b</sup>Kanazawa University, Kanazawa, Ishikawa, Japan

<sup>c</sup>Tokyo Metropolitan University, Hachioji, Tokyo, Japan

<sup>d</sup>University of Wisconsin, Madison, Wisconsin, United States

<sup>e</sup>Institute of Space and Astronautical Science, JAXA, Sagihara, Kanagawa, Japan

<sup>f</sup>Tohoku University, Sendai, Miyagi, Japan

<sup>g</sup>Yale University, Physics Department, New Haven, Connecticut, United States

<sup>h</sup>Sumitomo Heavy Industries, Ltd., Niihama, Ehime, Japan

**Abstract.** The Soft X-ray Spectrometer (SXS) is the first space-based instrument to implement operational redundancy of a sub-Kelvin cooling system. Its cooling system includes a superfluid helium cryostat and five cryocoolers, provided by Japan Aerospace Exploration Agency, and three adiabatic demagnetization refrigerators (ADRs) with four active heat switches, provided by NASA. These elements are configured in one of two ways to control the heat sink of the x-ray microcalorimeter detectors at 50 mK. The “helium mode,” the simpler of the two modes, is used while liquid helium is present and uses all five cryocoolers and two ADRs. The first two ADR stages operate together and reject their heat directly to the liquid at  $\sim 1.1$  K. In the “cryogen-free mode,” for operation after the helium is depleted, the first stage ADR operation is unchanged, the second stage is repurposed to control the empty helium tank at  $\sim 1.5$  K, and the third stage transfers heat from the 1.5-K stage to the 4.5-K interface of the Joule–Thomson cooler. The development and verification details of this capability are presented within this paper and offer valuable insights into the challenges, successes, and lessons that can benefit other missions, particularly those employing cryogen-free or hybrid cooling systems. © The Authors.

Published by SPIE under a Creative Commons Attribution 3.0 Unported License. Distribution or reproduction of this work in whole or in part requires full attribution of the original publication, including its DOI. [DOI: [10.1117/1.JATIS.4.2.021408](https://doi.org/10.1117/1.JATIS.4.2.021408)]

Keywords: Astro-H; Soft X-ray Spectrometer; cryogen free; cryocooler; cryogenic; cooling system; magnetic refrigeration; adiabatic demagnetization refrigerator.

Paper 17056SSP received Aug. 15, 2017; accepted for publication Feb. 22, 2018; published online Apr. 28, 2018.

## 1 Introduction

The Astro-H (Hitomi) mission<sup>1,2</sup> hosted the Soft X-ray Spectrometer (SXS) instrument,<sup>3,4</sup> a high-resolution cryogenic spectrometer featuring an x-ray microcalorimeter detector array operated at 50 mK. The SXS instrument is the collaborative product of NASA/Goddard Space Flight Center and Institute of Space and Astronautical Science/Japan Aerospace Exploration Agency (JAXA) with contributions from Netherlands Institute for Space Research and European Space Agency. The SXS instrument block diagram shown in Fig. 1 highlights the international contributions.

After the successful launch by JAXA’s 30th H2A rocket on February 17, 2016, the Astro-H observatory was renamed Hitomi. SXS was launched with 36 L of liquid helium aboard and achieved 50 mK on the fifth mission day after having successfully completed its prerequisite functional verifications.<sup>5</sup> The SXS was operated in its helium mode with performance closely matching that observed during ground tests.<sup>6–10</sup> Based on initial in-orbit measurements, the helium supply was expected to last about 4 years,<sup>9–12</sup> after which the SXS cooling system would be reconfigured for cryogen-free operation. By

mid-March 2016, the required SXS commissioning activities were complete except for the final task of opening the dewar gate valve to give the SXS detectors an unobstructed view of the sky through their x-ray optics.<sup>13</sup>

On March 26, 2016, the Hitomi satellite suffered a catastrophic loss of attitude control, loss of communication, and spacecraft breakup.<sup>2,5</sup> At the time, the cause of the communications loss was not known, and an eventual recovery still seemed plausible. Regardless of how long it might take, and however unlikely it was, if Hitomi were to be recovered, the SXS instrument could have been recovered too. Though the SXS helium supply only lasts a few weeks without power to run the cryocoolers, it had already been shown that the cooling system could be cooled from room temperature and successfully operated without cryogenics. Later as more details emerged, it became clear that Hitomi was indeed lost, a major setback to the mission science objectives.

The cryogen-free mode was not operated in space, but it was qualified for flight before launch and the necessary hardware functions were all verified in orbit. The development of this hybrid cooling system with independent operational modes has yielded important lessons, which are shared in this paper to benefit future missions employing exclusively cryogen-free or hybrid cryogen/cryogen-free cooling systems.

\*Address all correspondence to: Gary A. Sneiderman, E-Mail: [Gary.A.Sneiderman@nasa.gov](mailto:Gary.A.Sneiderman@nasa.gov)

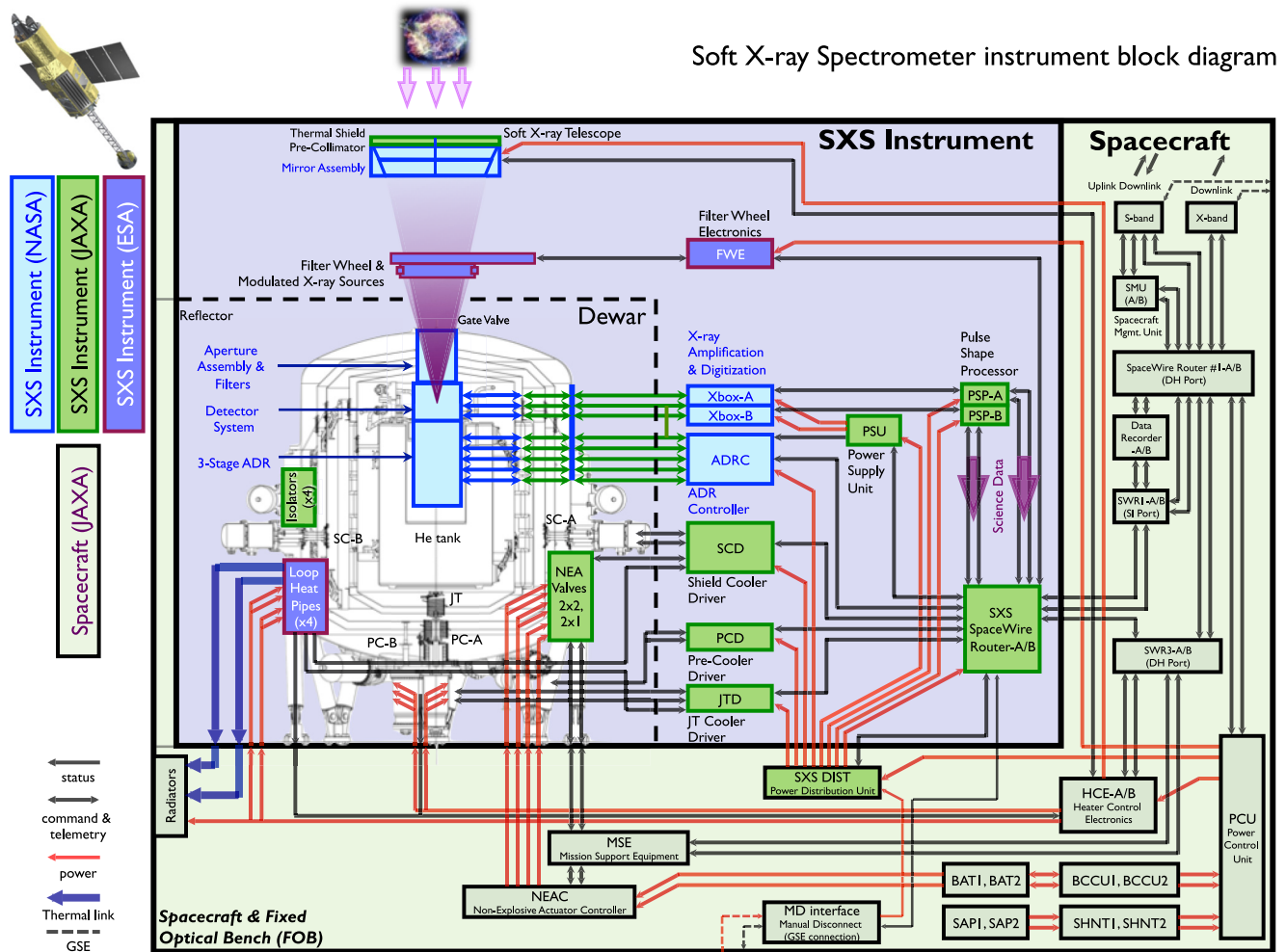


Fig. 1 SXS instrument block diagram.

## 2 Driving Performance Requirements

The SXS cooling system<sup>14–16</sup> is designed to satisfy the following driving requirements.

### 2.1 Overall Instrument Performance

The SXS x-ray spectrometer uses an array of 36 spatially and spectrally independent detector channels to measure x-ray photon energies with high-spectral resolution from across a broad x-ray band (0.1 to 12 keV). Spectral resolution is the primary performance characteristic of the spectrometer and most performance requirements derive from this requirement: the SXS shall measure x-rays to a spectral resolution of  $\leq 7$  eV FWHM. The peak temperature of the detectors corresponds to the energy of the x-ray photons they absorb.<sup>17</sup> Since the deposited energy of individual photons is tiny, the detectors must be extremely cold to measure the temperature response, and the reference temperature from which the response is measured must be extremely stable to obtain a precise measurement of the peak value. The requirements summarized below are imposed on the cooling system to enable the SXS to achieve these exquisitely sensitive measurements.

### 2.2 Detector Heat Sink Temperature and Stability

Measuring the temperature response to the absorption of individual x-ray photons requires an extremely cold detector.

## Soft X-ray Spectrometer instrument block diagram

During science observations, the cooling system shall maintain the detector heat sink at 50 mK. Accurate determination of the peak value of that temperature response requires precision temperature control. During science observations, the cooling system shall stabilize the heat sink temperature to  $\leq 2.5\text{-}\mu\text{K}$  RMS at 50 mK.

### 2.3 He Tank Temperature and Stability

The detectors are packaged inside their heat sink known as the calorimeter thermal sink (CTS). The CTS is mechanically connected to the detector assembly (DA) by a Kevlar suspension system and electrically connected to the DA through fine signal wires. The DA is mounted to the helium tank assembly, making the CTS sensitive to variability in the helium tank temperature through parasitic conductive effects. To keep these effects acceptably small, a requirement is imposed to stabilize the DA interface (helium tank) temperature to  $\leq 1\text{-mK}$  RMS during science observations.

### 2.4 Lifetime and Operational Duty Cycle

The mission requires a design lifetime  $\geq 3$  years. This time is sufficient to accomplish a specific set of baseline science measurements, after which the observatory is made available to the broader x-ray astronomy community. The baseline science

measurements are nominally completed within the first six months following completion of the in-orbit checkout activities. An overall mission efficiency of 40% is assumed to account for periods of Earth occultation, satellite maneuvers, data loss, and other activities unrelated to the SXS. From this, the following instrument duty cycle requirement is derived: the SXS shall be available for science observation  $\geq 90\%$  of the time. With this requirement, “available for science observation” means the temperature and stability requirements above are simultaneously satisfied. Conservatively, the net observing efficiency would be  $40\% \times 90\% = 36\%$ .

### 2.5 Stable Autonomous Operation

The mission is designed for a low-Earth circular orbit using a single primary ground station nominally staffed six days per week. This means that the SXS operation must be autonomous and stable for periods longer than 24 h.

### 2.6 Cryogen-Free Operation

The SXS must be able to accomplish its science operations, even without the presence of liquid helium. In other words, the requirements above must be satisfied with or without the liquid helium cryogen. This requirement was adopted for SXS in

response to the premature loss of cryogen from its predecessor instrument, the X-Ray Spectrometer,<sup>18</sup> flown aboard Suzaku.

## 3 Cooling System Overview

To satisfy the above requirements, the SXS cooling system is designed for operation in two different configurations, “helium mode” and “cryogen-free mode,” corresponding to the presence or absence of the liquid cryogen loaded into the system before launch. Figure 2 shows this cooling system and its complex arrangement of both active and passive cooling elements, including four 20-K 2-stage Stirling cryocoolers (2ST),<sup>19</sup> a 4.5-K Joule–Thomson (JT) cryocooler,<sup>19</sup> a 40-L superfluid helium tank, and 3-stage adiabatic demagnetization refrigerator (ADR).<sup>9</sup> When integrated, these elements are nested within a multistage dewar featuring four helium vapor cooled shields: outer, middle, and inner (OVCS, MVCS, and IVCS), and the innermost JT shield surrounding the helium tank. In addition to passive cooling from the helium effluent when present, a pair of 2ST coolers actively cools the OVCS and IVCS. The JT shield is actively cooled to 4.5 K by the JT cooler, assisted by another pair of 2ST coolers. This arrangement results in extremely low parasitic heat load to the helium tank ( $\sim 0.2$  mW) and satisfies the 3-year lifetime requirement with  $>30$  L of liquid.

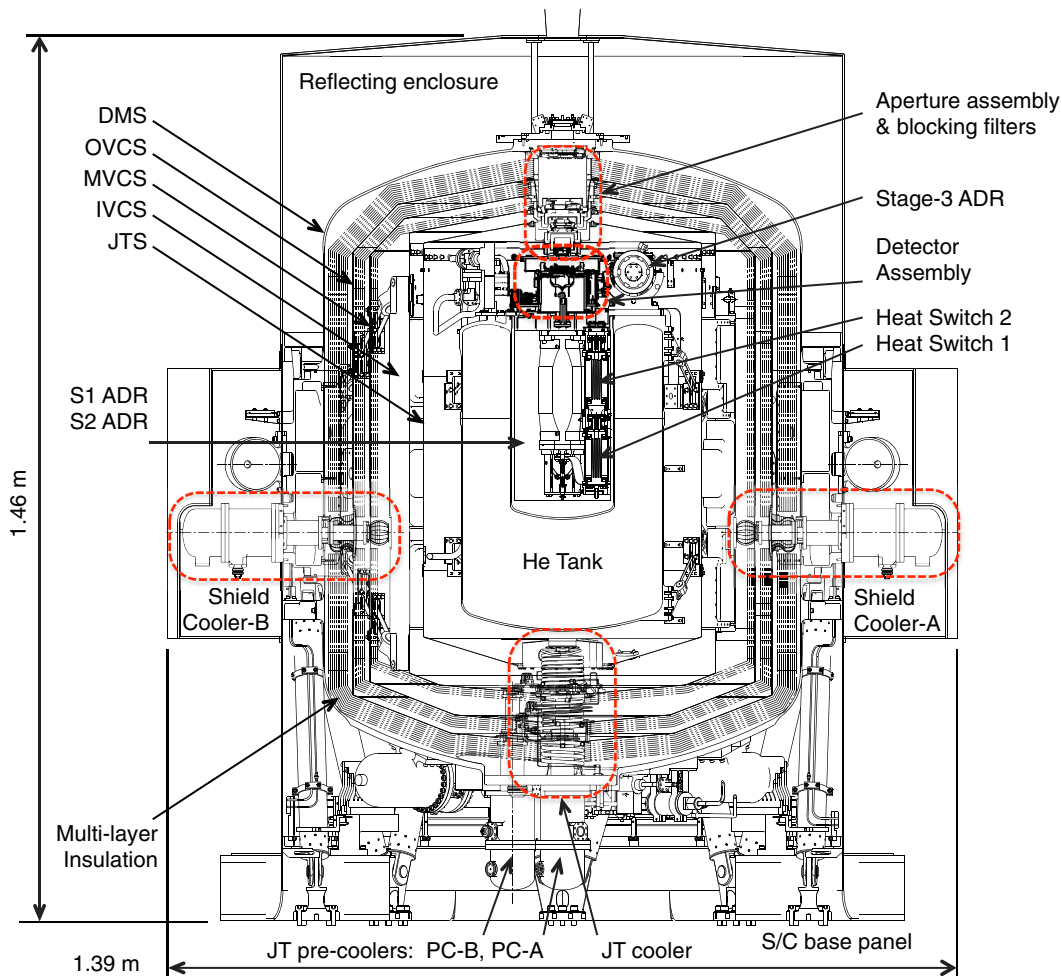


Fig. 2 Cross-sectional view of the SXS dewar.

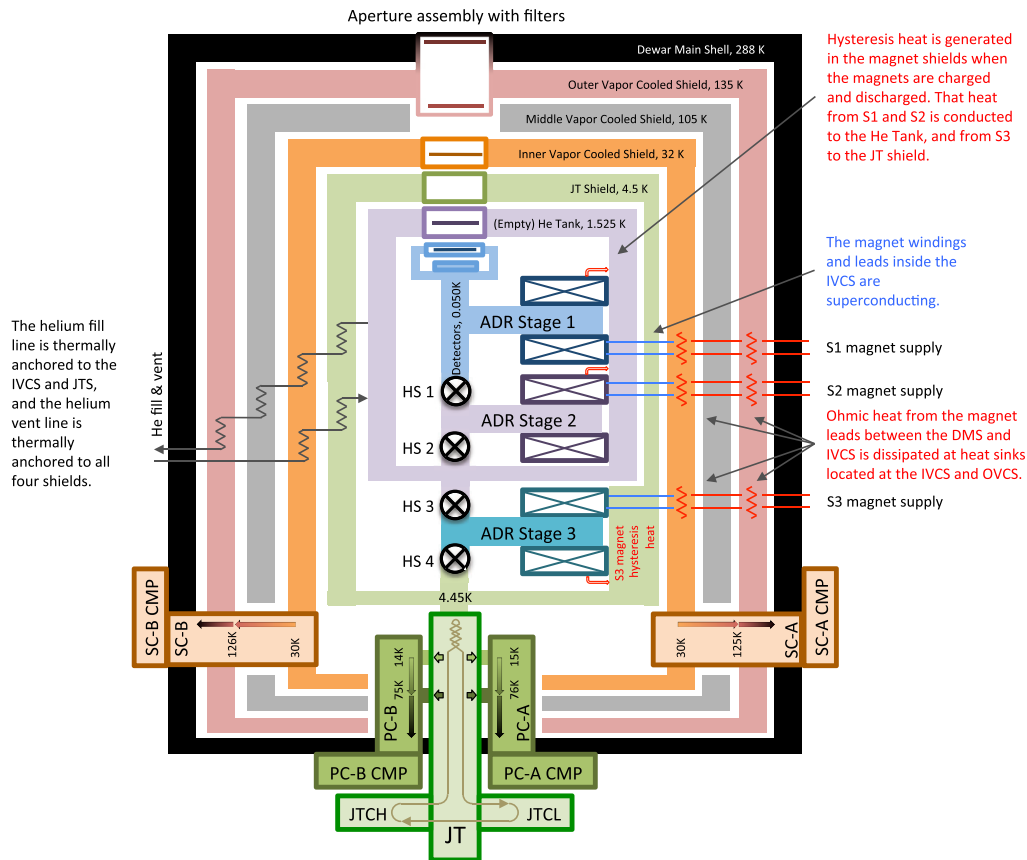


Fig. 3 SXS cooling system block diagram, including approximate cryogen-free equilibrium temperatures.

The detectors are mounted within their 50-mK heat sink, hereafter called the CTS. The CTS is mechanically supported by a Kevlar assembly from the ~1.3-K DA<sup>20</sup> and connected thermally to the ADR by flexible thermal foils. A package of four germanium resistance thermometers, used for 50-mK control and temperature monitoring, are integral to the CTS. The ADR includes three shielded magnet assemblies, each with a suspended paramagnetic salt assembly along its center, a series of thermal straps, and four heater actuated gas-gap heat switches (HS1 through HS4) to manage heat flows by thermally connecting or isolating the ADR stages and their heat sinks. With this

configuration, as shown in Fig. 3, the ADR controls the CTS at 50 mK using either the ~1.3-K liquid helium or the 4.5-K JT cooler as its heat sink. The ADR and DA are integrated as a single assembly called the calorimeter spectrometer insert (CSI), which is mounted to the top end of the helium tank to position the detectors at the focus of the instrument’s grazing-incidence x-ray mirror assembly. The closeout photo in Fig. 4 shows the hardware configuration.

#### 4 Driving Functional Requirements for Space Operation

The cryogenic system is designed to satisfy its requirements according to the following mission scenario. The instrument is launched with a full tank (>30 L) of superfluid helium, which evaporates slowly over a predicted lifetime of 3 years. During this period, the cryogenic system is operated in the helium mode where the first two ADR stages (S1 and S2) cool and stabilize the CTS at 50 mK, recycling periodically in single-shot manner using the liquid helium as a heat sink. In this case, the high heat capacity of the liquid passively stabilizes the helium tank and with it the DA. The system is operated in this mode for as long as liquid helium remains.

Once the helium is depleted (either at the end of its natural lifetime or prematurely due to an anomaly), the cooling system is reconfigured to use the JT stage as the ADR heat sink. In this case, the S3 and S2 ADR continuously cool the empty helium tank and stabilize the DA temperature, while the S1 ADR cools and stabilizes the CTS at 50 mK in a single-shot operation.

The cryogen-free operation is only useful if it can be started from a wide range of initial conditions. In the worst case, the

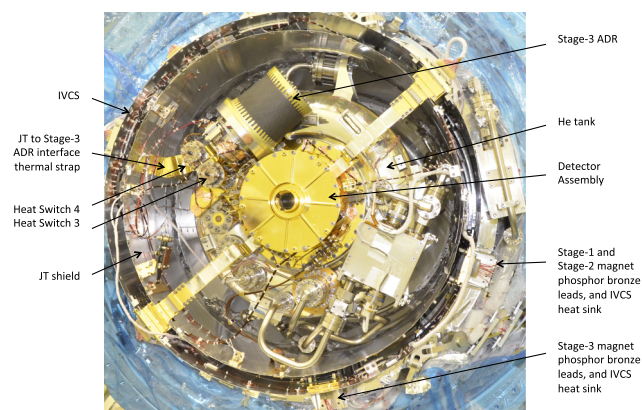


Fig. 4 Closeout photo of the forward interior portion of the SXS dewar.

entire system begins at room temperature with no liquid helium. Two capabilities are, therefore, required:

1. The cryocoolers' must be able to cool down from room temperature and bring the JT stage, helium tank, ADRs, and DA into equilibrium at 4.5 K (the starting point for #2).
2. The ADRs' must be able to and cool from 4.5 K (the end point of #1) to nominal operating conditions with the CTS at 50 mK.

The first capability was demonstrated by test using the high-fidelity engineering model of the complete dewar,<sup>21</sup> and all cryogen-free tests began at the 4.5-K equilibrium state, so the second capability was demonstrated each time cryogen-free tests were conducted.

## 5 Ground Test Campaign Approach

All of the final instrument tests occurred in Japan, so many of the SXS team members supported these while on international travel. To accommodate the advanced needs for travel, the tests were organized into campaigns, typically lasting 10 to 14 days. These campaigns began with a warm system. A standardized procedure cooled the dewar (3 days) and completed a series of functional and performance verification tests (1 day). Upon completion, the cooling system is configured with an approximately half-full tank of liquid helium at 1.3 K, all coolers running, and the ADRs operating in the helium mode. Once testing with liquid cryogen is finished, the helium is evaporated either as the first step toward a full warm-up or to reconfigure for cryogen-free tests.

When reconfiguring for cryogen-free testing, the helium is evaporated more slowly to avoid thermal overshoot once the liquid is gone. Then the system is re-cooled to 4.5 K with cryocoolers. The helium evaporation and 4.5-K recovery take 24 h.

At 4.5 K, the ADR cryogen-free operations begin next, starting with S3. The S3 ADR is cycled to remove heat from the colder stages and transfer it to the JT. A while later, operation of the S1 and S2 ADR begins. As S3 cools, the system S1 and S2 will begin charging. Eventually, S1 and S2 have enough cooling capacity to complete their cycle and cool to 50 mK. This initial cool-down cycle takes between 6 and 8 h to reach 50 mK. The long initial cool-down affects the 50-mK hold time of this first cycle, and so the first cycle is not included when verifying nominal cryogen-free performance. Once this first cycle completes and the next S1 recycle begins (~17 h after 50 mK is first reached), the ADRs operate with a repeating cycle pattern and very little variation in 50-mK hold time, S1 recycle time, and S2 and S1 starting current after the S1 recycle.

When started at 4.5 K, nominal operating conditions can be reached within 1 day. But, as we recognized later, the same is not true of the dewar—it has a much longer time constant that prevents the system from reaching equilibrium until much later. Failing to recognize that fact was at the root of the cryogen-free development challenges. The test campaigns were not long enough, and verification tests of the cryogen-free operation were conducted before the dewar itself had equilibrated.

## 6 Cooling System Operation History

A high-fidelity engineering model of this system was completed about two years earlier than the flight model and was to be the primary test platform for verification and validation and

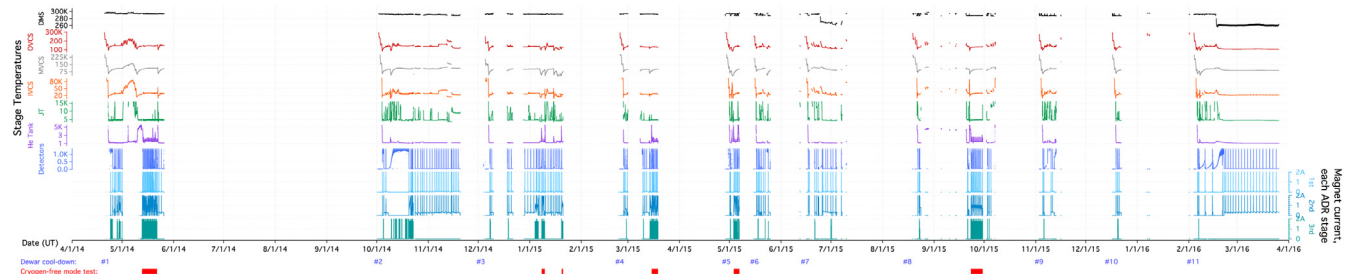


Fig. 5 Operational history of the flight SXS dewar. The red bars at the bottom indicate cryogen-free tests.

Table 1 The cryogen-free test campaigns of SXS.

Test	Purpose	Date(s)	Duration (h)
1	Self-compatibility and initial parametric tests (early tests conducted before the flight dewar was completed)	May 13 to 21, 2014	217
2	Parameter and functional checks	January 8 to 10, 2015	45
3	Quick check of detector noise without LHe before warm-up	January 20, 2015	21
4	Performance evaluation, operation during SXS calibration <sup>20</sup>	March 15 to 19, 2015	94
5	Demonstration of operation, #1	May 3 to 6, 2015	72
6a	Demonstration of operation, #2	September 23 to 30, 2015	170
6b	Stability test (subset of test 6)	September 25 to 29, 2015	104

for demonstrating the operation and control strategies. Unfortunately, hardware anomalies within that system severely limited its usefulness. Before the flight system was completed, the cryogen-free mode had only been tested with the CSI integrated into a nonflight dewar configured with flight-like interface temperatures but with different dynamic thermal responses. This system was sufficient to demonstrate the ADR hardware functions and the performance of its components but was too different from the flight environment to be used for control algorithm validation.

A timeline of the complete operational history of the flight system, from its first cool-down to the final telemetry received from the instrument in orbit, is provided in Fig. 5. The figure shows the temperature of each stage and current in each ADR magnet. The flight SXS cooling system was cooled from room temperature to 50 mK, 11 times before launch and operated for a total 4367 h. The CTS was controlled at 50 mK for more than 2900 h. The system was operated in the cryogen-free

mode only six times, as listed in Table 1. Those tests represent a small fraction of the total operating time, but they were crucial as they provided the only means by which the operating mode could be refined and verified. These six tests yielded important insights that eventually led to a successful control strategy.

## 7 Cryogen-Free Operational Design

### 7.1 Basic Operation

In cryogen-free mode, the ADR performs two separate functions. The first is continuous cooling of the helium tank, and the second is single-shot cooling of the detector array. Cooling of the helium tank is accomplished by rapidly cycling S3 between the JT and helium tank temperatures to absorb heat from the tank and reject heat to the JT. During the S3 cycle, HS4 and HS3 are alternately actuated to connect or isolate the JT or the helium tank to S3. Meanwhile HS2 remains powered, except during recycling of S1, connecting S2 with the helium tank. This

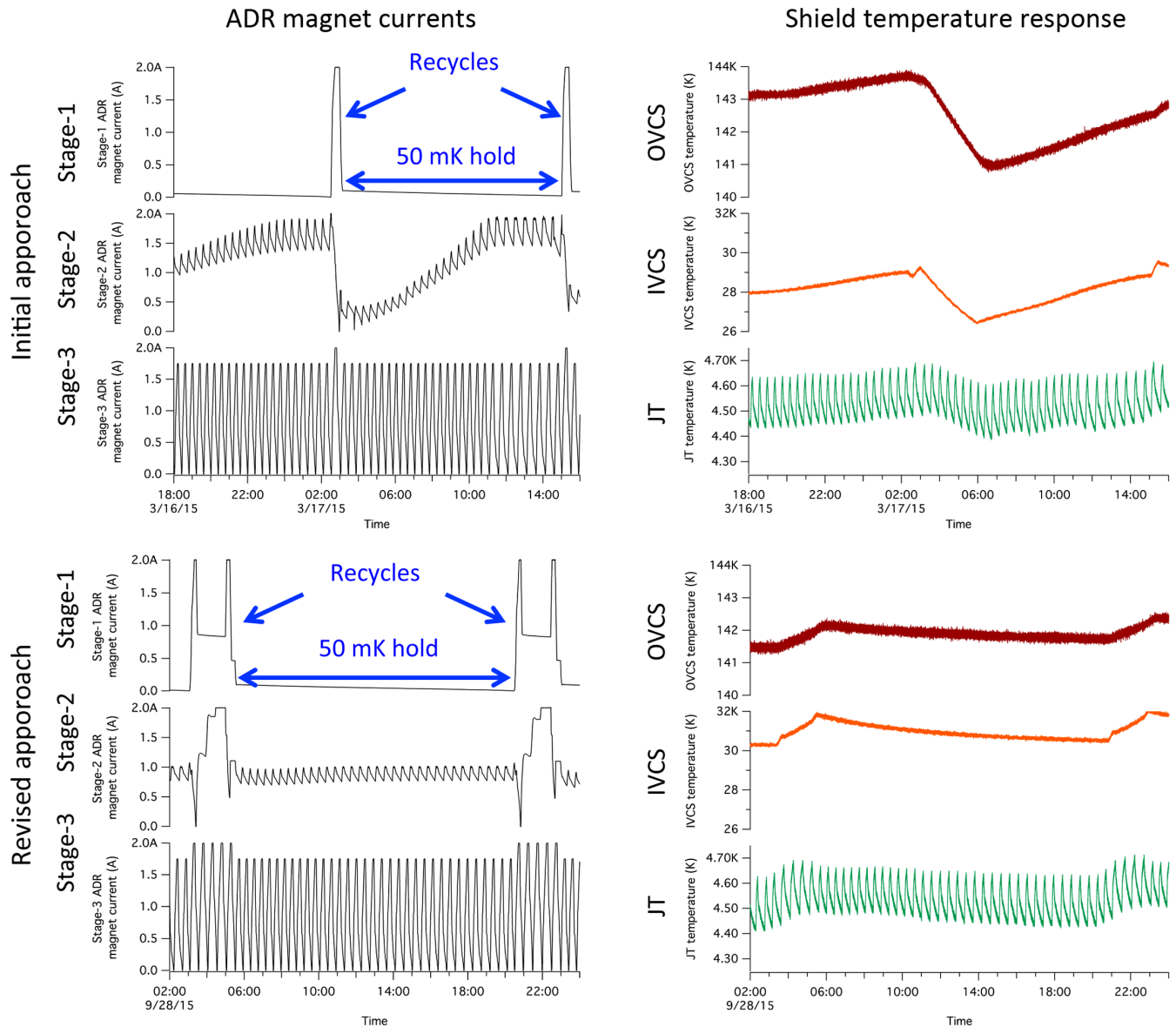


Fig. 6 Magnet current profiles and shield temperature responses with the original and revised ADR control algorithms.

allows S2 to function as an active heat capacity and stabilize the tank temperature at  $\sim 1.5$  K. It does this by absorbing the tank's parasitic heat load when S3 is isolated by HS3 and pushing that heat out to S3 when HS3 is on and the two stages are connected. The S1 operates in the usual manner for a single-shot stage; it provides detector cooling for a period of time, then recycles by rejecting heat to S2 (which stores and rejects that heat over time to S3).

The main difference for S1 in the cryogen-free mode, compared with the helium mode, is that S2 is warmer in the cryogen-free mode during the S1 hold time ( $\sim 1.5$  versus  $0.5$  K). This increases the parasitic load on S1 through HS1 ( $\sim 1.3$  versus  $0.05 \mu\text{W}$ ), which reduces the S1 hold time to about 15 h compared with 48 h in the helium mode. To satisfy the observing efficiency requirement (90%) with a much shorter hold time, the S1 recycle time must to be kept to a fraction of an hour.

Unlike the helium mode, in the cryogen-free mode, all of the heat resulting from the ADR operation is absorbed by cryo-coolers and rejected to space by radiators. The heat generated by the ADR itself (heat from the salt pills, hysteresis heat from the magnets, and dissipation in the heat switch getter heaters) is absorbed by the JT cooler and passed on to the precoolers, and the ohmic heat generated in the resistive portion of the magnet leads during ADR operation is absorbed by the shield coolers (see Fig. 3).

Because S1 is operated at a lower average current than the other stages, its magnet leads were designed with higher electrical resistance than the others to minimize the total (conducted and generated) heat of the ADR magnet leads. As a result, the operation of S1 produces more ohmic heating than S2 or S3 at equivalent current. The instantaneous worst case occurs during the S1 recycle while S1 and S2 are both operated at elevated current. This was not initially anticipated to have a significant effect on the ADR operation or its heat sink, the JT cooler. But the cryocoolers are operated at fixed voltages; so additional loads raise the shield temperatures, thereby increasing the heat load onto the JT cooler and, through the CSI, onto the helium tank. This circumstance sets up the following critical point in the operation.

Having just absorbed S1's heat during its recycle, the stored cooling capacity in S2 after the S1 recycle is reduced, yet it needs to continue absorbing the helium tank's parasitic heat (which is also at its highest in this timeframe). Excess load on the JT raises its temperature and slows the S3 heat transfer prolonging the time before S3 can again extract heat from the helium tank and begin to charge S2 with its excess cooling capacity. If the S2 current ever becomes too low ( $< \sim 50$  mA), temperature control will be lost and the helium tank will warm—a condition from which the ADRs cannot automatically recover. The problem is that after the S1 recycle, the system requires the highest cooling power from the S2 ADR to regain temperature control of the helium tank at the same time as its cooling power is at its lowest ebb.

The original approach to cryogen-free operation<sup>22</sup> was to gradually build up cooling capacity in S2 over the 50-mK hold and then fully absorb the heat stored in S1 in a single-shot recycle. This can be achieved if the combined S2 and S3 cooling powers exceed the parasitic heat load to the helium tank with enough margin (a few tenths of a mW). Early ground tests confirmed this; when the JT and shield coolers are operated at their nominal voltages, they maintained the IVCS and JT shields at sufficiently low temperature ( $\sim 30$  and  $4.3$  K). The characteristic profile of this cycling process can be seen in the top half of Fig. 6 where the increasing cooling capacity stored in S2 over multiple S3 cycles is manifest as a rising S2 current.

Unfortunately, the early tests of cryogen-free mode were conducted with more favorable conditions than would exist in flight. The configuration change to set up cryogen-free testing required boiling off significant quantities of liquid helium, which overcooled the shields. This was overcome by operating the cryocoolers at reduced power until the shields warmed to their nominal temperature ranges. The oversight was the effect of the overcooled MVCS, which is isolated from the coolers and recovers with a long time constant of  $\sim 10$  days. At equilibrium, the MVCS temperature is over 106 K, and at that temperature, its heat load onto the IVCS represents half of the total IVCS load. With the unrecognized exception of the MVCS temperature, the other initial conditions were quickly met and cryogen-free

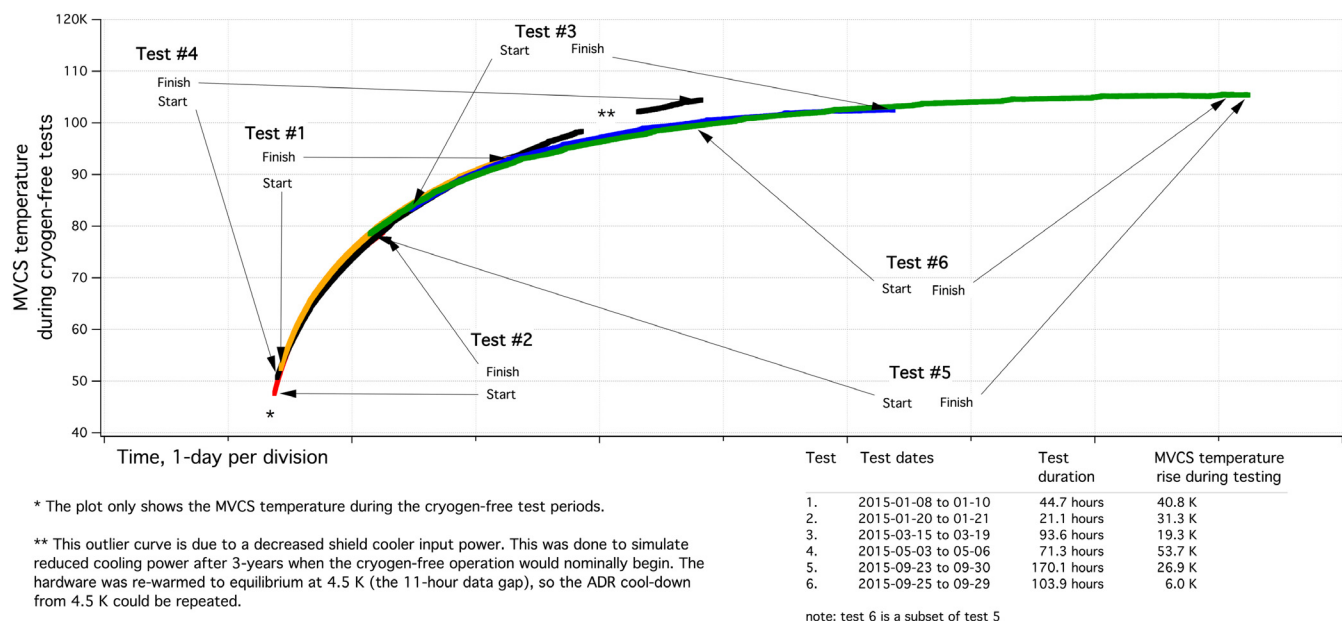


Fig. 7 MVCS warming during cryogen-free tests.

testing began. The tests proceeded as the MVCS warmed, exposing the colder stages to increasing heat loads during the tests. The evolution of heat loads, masked by the ADRs dynamic loading of the shields, was not noticed. What was observed was an inability to maintain temperature control of the helium tank after S1 recycles because the stored cooling capacity of S2 was too low at that point. Figure 7 shows how much the MVCS temperature changed during the cryogen-free tests.

In subsequent, longer-term tests, it became clear that as the system approached equilibrium, the previously envisioned approach to cryogen-free operation was not stable and a different operating strategy, one that is stable at equilibrium conditions, was needed. But, accomplishing that required new priorities among the performance requirements and agreement on which could be compromised. The conclusion that stable operation was more important than observing efficiency created a pathway to an acceptable solution.

## 7.2 Revised Cryogen-Free Mode Operation

Through modeling and simulation, it was determined that the key indicator of stable ADR operation was the IVCS temperature variability, and the ADR's operation and control algorithm was revised to minimize excursions in the IVCS temperature. The mechanism for doing this was to minimize variations in the ADR's magnet currents, and the principal change was to limit the maximum current that S2 could build up to (1 A instead of 2 A) as S3 cycled. The penalty was that at this lower current S2 could not store enough cooling capacity to recycle S1 in a single

transfer of heat. Instead, when S1 required recycling, S2 would absorb heat until its capacity was depleted, then it would be warmed to a relatively high temperature of 2.5 K where S3 could rapidly rebuild its cooling capacity. Once S2 was charged at 2.5 K, it was cooled down to 0.8 K where it could fully recycle S1, allowing it to demagnetize to 50 mK and begin a new hold time.

The algorithm required a much longer S1 recycle time, on the order of 2.5 h, which reduced the duty cycle to 84%. The gain was in reliability, in the form of an ability to recycle S1 regardless of the prevailing JT and IVCS temperatures associated with their nominal operating voltages.

Before a test campaign could be approved to test this modification, it was necessary to demonstrate through simulations that the algorithm achieved the desired level of stability even if the cryogenic system (OVCS, MVCS, and IVCS) warmed during its approach to equilibrium. A high-fidelity model was constructed,<sup>23</sup> which merged a previous model of the ADR<sup>24</sup> with models of how the JT and shield coolers and the vapor cooled shields responded to ohmic heat inputs. The resulting model was able to predict the time evolution of the OVCS, MVCS, and IVCS temperatures and transient response of the JT cryocooler as the ADR model generated instantaneous heat loads produced by its operation. The resulting modeled behavior agreed with measured MVCS, IVCS, and JT temperatures from previous tests.

Based on the success of the integrated modeling effort and good correlation with past test results, as well as a fortuitous unplanned break in the project schedule, an additional

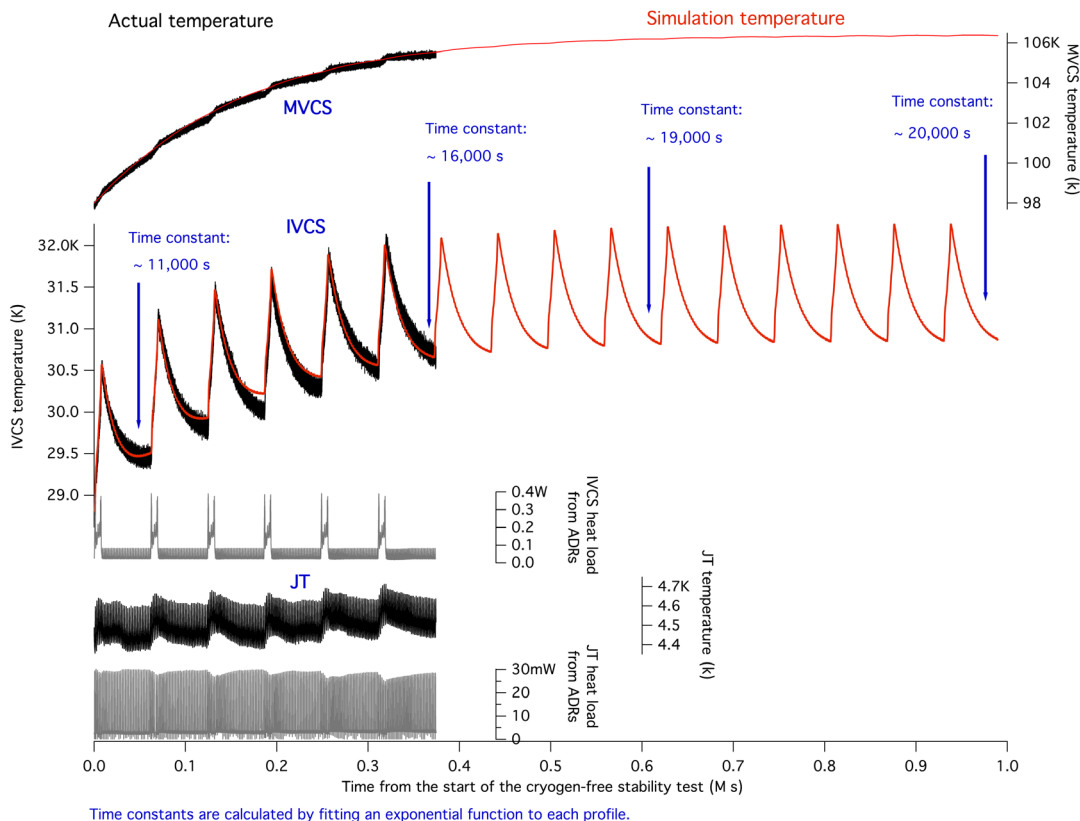


**Fig. 8** Modeled versus measured MVCS and IVCS temperatures during the stability test and the calculated ADR generated heat loads on the IVCS and JT. The time constants indicated in this figure represent the cool-down rate of the IVCS among S1 recycles.

cryogen-free mode test campaign was approved by the project. The purpose of the new test was to obtain the data necessary to validate and correlate the updated model, and if time permitted to demonstrate the anticipated stable autonomous operation as the system approached equilibrium. Stable autonomous operation meant that once the setup was complete, no commands would be sent to the instrument. These tests would run as long as possible up to an agreed deadline when control of the spacecraft had to be returned to the project.

Using the modified algorithm, testing began with the initial cooldown from 4.5 K to 50 mK, which completed successfully after 6 h. That was followed by two days of engineering evaluations of the updated algorithms. Then the stability test began after the end of a normally completed cycle. The stability test demonstrated that the performance of the SXS instrument in the final cryogen-free mode was stable and required no human intervention even as the dewar warmed and approached equilibrium. Six ADR cycles were completed during this autonomous operating period lasting 104 h before ending in time to meet the agreed test deadline. Figure 8 compares the modeled prediction with the measured MVCS and IVCS temperatures, and Fig. 9 shows the same comparison for all stages over a longer time scale, demonstrating how the stable operation would continue. Demonstrating the repeatability of the system during cryogen-free operation, Fig. 10 shows an overlay of the current in S1's magnet during the six hold times of this test. Long-term variations in the heat load to S1 would cause the time base for each hold time to be compressed or elongated. Instead, the exact overlap of all six cycles indicates that the helium tank temperature was maintained at a constant, and the same, value (1.525 K) during all six cycles. Moreover, long-term variations in IVCS and JT temperature did not affect the ability of S1 and S2 to maintain the detectors and helium tank at stable temperatures.

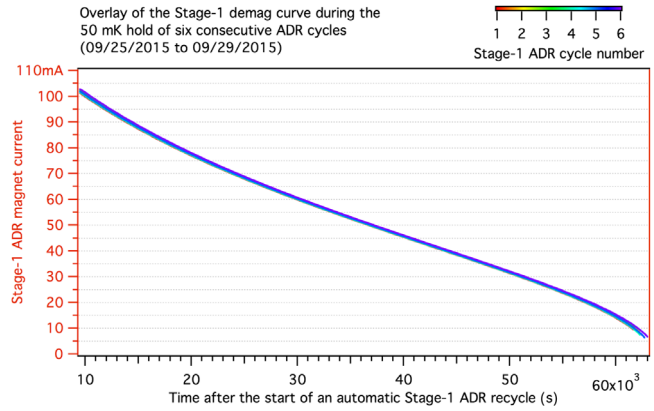


**Fig. 10** Overlay plot of the S1 magnet current profile during the six 50-mK hold periods of the stability test.

During the science observation periods of this test, the detector heat sink was controlled at 50 mK with a stability of  $<0.8\text{-}\mu\text{K}$  RMS, meeting the requirement of  $<2.5\text{-}\mu\text{K}$  RMS, and during the same time periods, the DA thermal gasket (He tank) was controlled at 1.525 K with a stability of  $<520\text{-}\mu\text{K}$  RMS, meeting the requirement of  $<1\text{-mK}$  RMS. These results are shown in Fig. 11.

An operational efficiency of 84% was achieved with consistent 2.5-h-long recycle periods, 18-min detector equilibration durations at 50 mK, and 14.7-h-long periods with stable control at 50 mK. With the temperatures well controlled, the instrument achieved a composite spectral resolution of 4.3 eV FWHM showing that the instrument's spectral resolution is unaffected by differences between the two operating modes. Table 2 compares requirements with measured performance in the cryogen-free and helium modes.

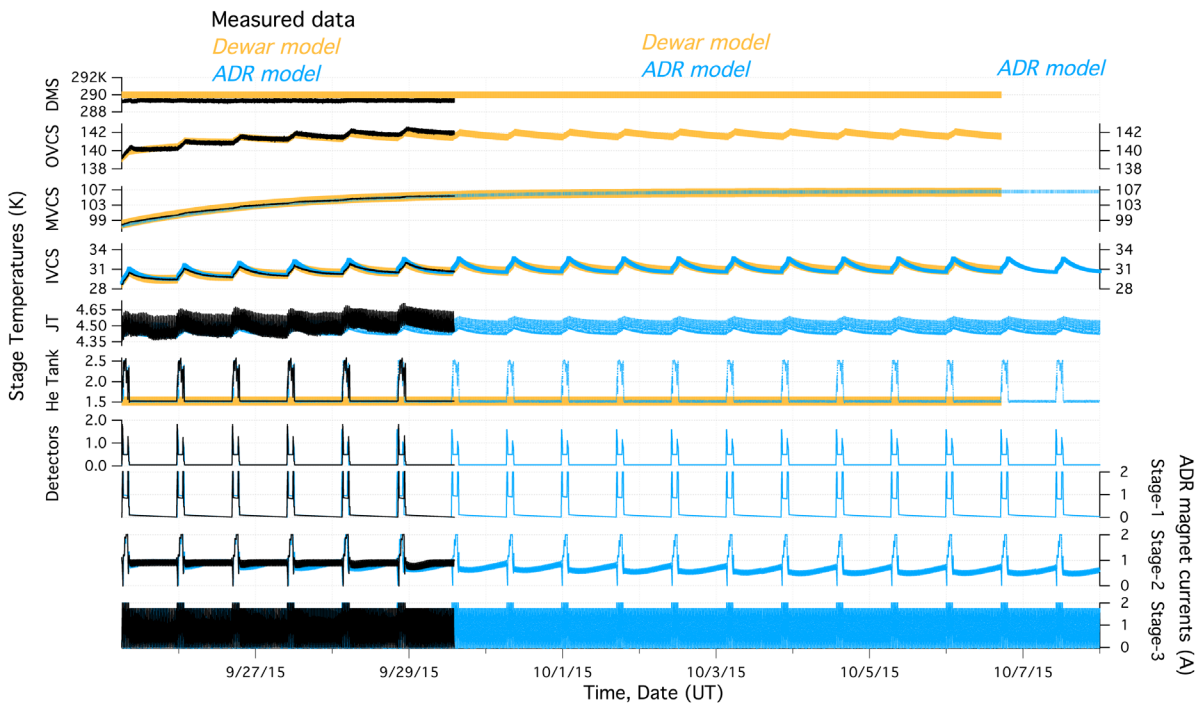


**Fig. 9** Modeled versus measured stage temperatures and magnet currents during the stability test and predicted results thereafter.

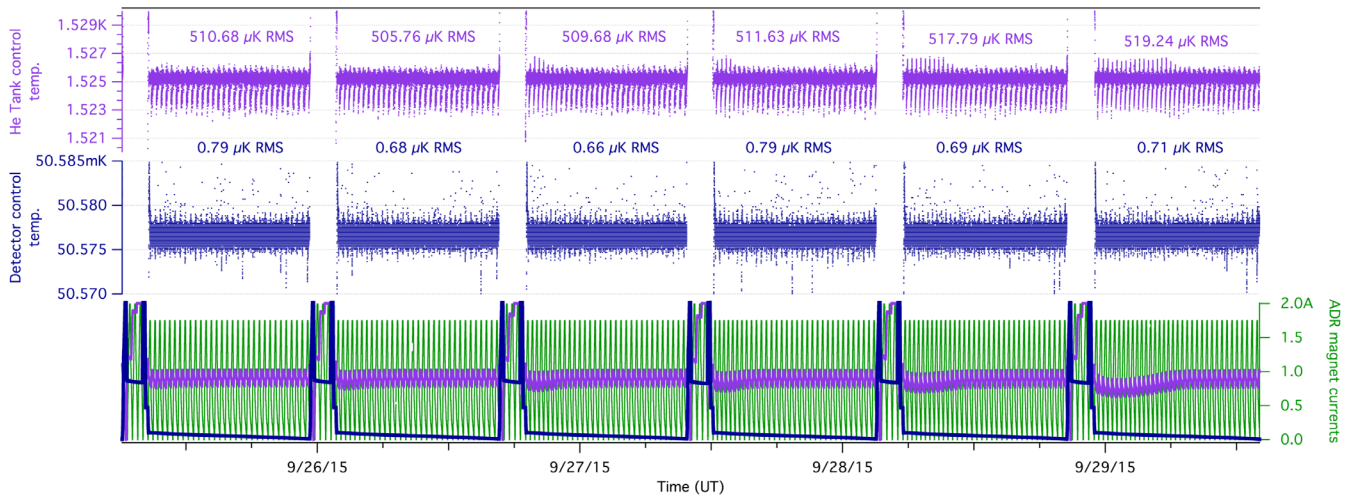


**Fig. 11** Temperature stability performance during the stability test, requirements are: detectors  $\leq 2.5\text{-}\mu\text{K}$  RMS at 50 mK and helium tank  $\leq 1\text{-mK}$  RMS at  $< 1.8\text{ K}$ .

**Table 2** Requirements and measured performance of the SXS cooling system in its two science operating modes. Requirements not met are shown in parentheses.

Parameter	Cooling System Requirement	Cryogen-Free Mode	Helium Mode
Detector heat sink temperature (mK)	50	50	50
Detector heat sink temperature stability ( $\mu\text{K}$ RMS)	$\leq 2.5$	$\sim 0.75$	$\sim 0.4$
Helium tank temperature (K)	—	1.525	1.1 to 1.3
DA temperature stability (mK RMS)	$\leq 1$	0.5	0.6
Stage 2 temperature (K)	—	1.525	0.5
Stage 1 hold time at 50 mK (h)	—	14.53	$> 42.3$
Stage 1 recycle time (h)	—	2.49	0.57
Settling time at 50 mK (h)	—	0.30	0.35
Observing efficiency (%)	$\geq 90$	(84)	$> 97$
Autonomous operation (h)	$> 24$	$> 104$	$> 42$
Warm start from heat sink temperature	Required function	6 h from 4.5 K	1.1 h from 1.4 K
Instrument spectral resolution (eV FWHM)	$\geq 7$	4.3	4.4

## 8 Key Lessons

- i. With different parts of the cooling system developed separately by different organizations, the interdependent functions, such as cryogen-free operation, are difficult to test separately. An engineering model was developed for this reason, but internal hardware failures made that system inoperable for cryogen-free testing. The integrated thermal model proved to be a critical tool for evaluating the merits of alternative operational strategies and for simulating flight performance. If the system-level thermal model had been developed earlier, the effort to finalize the operational strategy could have converged much sooner.
- ii. Cryogen-free tests were scheduled after the other cryogen-based events, such as the cool-down from room temperature, hardware checkouts, and other planned tests. This is a very practical test order, but it created very long test campaigns that stressed the small SXS team. If the necessary duration of cryogen-free tests was recognized early, staffing or the test campaigns themselves could have been more efficiently planned.
- iii. The passive warm-up of the MVCS drove the schedule to configure the system for the cryogen-free mode. This could have been mitigated during the design phase, such as with the addition of a nonflight heater.

- iv. Failing to understand the effect of a cold MVCS meant cryogen-free tests were performed in unrealistically favorable conditions leading to problems with the originally designed operational approach. Fortunately, the root cause of the problems was recognized in time. But developing an approach and an integrated model to simulate it was unplanned and required some heroic efforts, and securing a sufficiently long test opportunity to validate the model required a bit of good fortune. This situation is best avoided in the planning phase by recognizing the details that form the exceptions to test-as-you-fly.

## 9 Conclusions

The Astro-H SXS instrument adopted the ambitious goal of creating a redundant cryogenic system, based on both stored cryogenics and cryocoolers, that could provide deep sub-Kelvin cooling (50 mK) of an x-ray microcalorimeter array. The relatively large difference in heat sink temperature that these two configurations provided for the operation of the ADR created a significant challenge. In the end, the cooling system was shown to provide the required cooling for both helium and cryogen-free modes.

Successful development of the cryogen-free mode algorithms depended in part on developing an integrated thermal model of the ADR and cryogenic system. This model was used to predict the long-term evolution of the full cryogenic system as it approached equilibrium with the ADRs operating and was ultimately validated by test of the flight system before launch. The resulting design significantly improved the repeatability and reliability of the ADR operation in the cryogen-free mode and provided stable control that could confidently be run autonomously. The cryogen-free mode of operation was not used in orbit, but its prelaunch demonstration in near-equilibrium conditions gives confidence that the SXS instrument would have operated as expected in its cryogen-free mode in-orbit.

## Acknowledgments

The authors are grateful to all of the SXS team members in the US, Japan, and Europe who devoted themselves to the success of the SXS instrument. We would like to specifically acknowledge the enduring dedication of those team members who also supported the X-Ray Spectrometer instruments that preceded the SXS for helping to bring forward the many lessons that contributed to the success of the SXS development. We acknowledge everyone at Sumitomo Heavy Industries, Ltd. who manufactured the SXS dewar. We also appreciate Dr. A. Okamoto, K. Ishikawa, and Y. Ezoe, for their contributions to the construction of the thermal model that was used for the cryogen-free test. We are grateful to the project for its support of the SXS instrument and its demanding test program, with particular gratitude for its understanding of the criticality of the final cryogen-free tests and for securing the opportunity to perform it.

## References

1. T. Takahashi et al., “The ASTRO-H X-ray astronomy satellite,” *Proc. SPIE* **9144**, 914425 (2014).
2. T. Takahashi et al., “The ASTRO-H (Hitomi) X-ray astronomy satellite,” *Proc. SPIE* **9905**, 99050U (2016).
3. R. L. Kelley et al., “The ASTRO-H high-resolution soft x-ray spectrometer,” *Proc. SPIE* **9905**, 99050V (2016).
4. K. Mitsuda et al., “Soft x-ray spectrometer (SXS): the high-resolution cryogenic spectrometer onboard ASTRO-H,” *Proc. SPIE* **9144**, 91442A (2014).
5. M. Tsujimoto et al., “In-orbit operation of the Astro-H SXS,” *Proc. SPIE* **9905**, 99050Y (2016).
6. C. A. Kilbourne et al., “The design, implementation, and performance of the ASTRO-H SXS calorimeter array and anti-coincidence detector,” *Proc. SPIE* **9905**, 99053L (2016).
7. F. S. Porter et al., “In-flight performance of the soft x-ray spectrometer detector system on Astro-H,” *Proc. SPIE* **9905**, 99050W (2016).
8. T. Okajima et al., “First peek of ASTRO-H soft x-ray telescope (SXT) in-orbit performance,” *Proc. SPIE* **9905**, 99050Z (2016).
9. P. J. Shirron et al., “Design and on-orbit operation of the adiabatic demagnetization refrigerator on the Astro-H soft x-ray spectrometer instrument,” *Proc. SPIE* **9905**, 99053O (2016).
10. R. Fujimoto et al., “Performance of the helium dewar and cryocoolers of Astro-H SXS,” *Proc. SPIE* **9905**, 99053S (2016).
11. Y. Ezoe et al., “Porous plug phase separator and superfluid film flow suppression system for the soft-x-ray spectrometer onboard ASTRO-H,” *Proc. SPIE* **9905**, 99053P (2016).
12. H. Noda et al., “Thermal analyses for initial operations of the soft x-ray spectrometer (SXS) onboard Astro-H,” *Proc. SPIE* **9905**, 99053R (2016).
13. Y. Soong et al., “ASTRO-H Soft X-ray telescope (SXT),” *Proc. SPIE* **9144**, 914428 (2014).
14. R. Fujimoto et al., “Cooling system for the soft X-ray spectrometer onboard Astro-H,” *Cryogenics* **50**, 488–493 (2010).
15. R. Fujimoto et al., “Cooling system for the soft x-ray spectrometer (SXS) onboard ASTRO-H,” *Proc. SPIE* **7732**, 77323H (2010).
16. S. Yoshida et al., “Flight model performance test results of a helium dewar for the soft X-ray spectrometer onboard ASTRO-H,” *Cryogenics* **74**, 10–16 (2016).
17. M. E. Eckart et al., “Ground calibration of the Astro-H soft x-ray spectrometer,” *Proc. SPIE* **9905**, 99053W (2016).
18. R. L. Kelley et al., “The Suzaku high resolution x-ray spectrometer,” *Publ. Astron. Soc. Jpn.* **59**, S77–S112 (2007).
19. Y. Sato et al., “Development status of the mechanical cryocoolers for the soft x-ray spectrometer on board Astro-H,” *Cryogenics* **64**, 182–188 (2014).
20. M. P. Chiao et al., “System design and implementation of the detector assembly of the Astro-H soft x-ray spectrometer,” *Proc. SPIE* **9905**, 99053M (2016).
21. K. Kanao, “Cryogen free cooling of ASTRO-H SXS helium dewar from 300 K to 4 K,” *Cryogenics* **88**, 143–146 (2017).
22. P. J. Shirron et al., “Design and predicted performance of the 3-stage ADR for the soft x-ray spectrometer instrument on Astro-H,” *Cryogenics* **52**, 165–171 (2012).
23. H. Noda et al., “Thermal analysis for initial operations of the soft X-ray spectrometer onboard the Hitomi satellite,” *J. Astron. Telesc. Instrum. Syst.* **4**(2), 011202 (2017).
24. P. J. Shirron et al., “Thermodynamic performance of the 3-stage ADR for the Astro-H soft x-ray spectrometer instrument,” *Cryogenics* **74**, 24–30 (2016).

Biographies for the authors are not available.